Annual Report for EM Science Program FY 1996 Award

Investigation Of Microscopic Radiation Damage In Waste Forms Using ODNMR and AEM Techniques

Guokui Liu

Chemistry Division, Argonne National Laboratory

September, 1997

Summary

This project seeks to understand the microscopic effects of radiation damage in nuclear waste forms. Our approach to this challenge encompasses studies in electron microscopy, laser spectroscopy, and computational modeling and simulation. During this first year of our project, our efforts have focused on a-decay induced microscopic damage in crystalline orthophosphates (YPO_4 and $LuPO_4$) that contain the short-lived α-emitting isotope ^{244}Cm ($t_{1/2}$=18.1 y). The samples that we studied were synthesized in 1980 and the initial ^{244}Cm concentration was ~1%. Studying these materials is of importance to nuclear waste management because of the opportunity to gain insight into accumulated radiation damage and the influence of aging on such damage. These factors are critical to the long-term performance of actual waste forms [1].

Lanthanide orthophosphates, including $LuPO_4$ and YPO_4, have been suggested as waste forms for high level nuclear waste [2] and potential hosts for excess weapons plutonium [3,4]. Our work is providing insight into the characteristics of these previously known "radiation-resistant" materials. We have observed loss of crystallinity (partial amorphization) as a direct consequence of prolonged exposure to intense alpha radiolysis in these materials. More importantly, our observation of microscopic cavities in these aged materials provides evidence of significant chemical decomposition that may be difficult to detect in the earlier stages of radiation damage. Our preliminary results show that, in characterizing crystalline compounds as high level nuclear waste forms, chemical decomposition effects may be more important than lattice amorphization which has been the focus of many previous studies. More extensive studies, including *in-situ* analysis of the dynamics of thermal annealing of self-radiation induced amorphization and cavity formation, will be conducted on these aged $^{244}Cm:LuPO_4$ and $^{244}Cm:YPO_4$ samples, along with other related compounds and glasses, in next two years of this project.

Analytical Electron Microscopy

The use of analytical electron microscopy (AEM) techniques is an important approach in our project in that it enables visualizing microscopic damage in the materials of interest. Whereas the electron diffraction (ED) patterns qualitatively determined the degree of amorphization in the samples that we investigated, transmission electron microscopic (TEM) images allowed us to visualize the microscopic structure damage and to observe nano-cavities in aged crystalline samples containing alpha-emitting isotopes. In contrast to the radiation damage simulation studies, such as heavy ion implantation of crystalline compounds [5-7], in our work on 17-year old orthophosphate crystals containing~1% ^{244}Cm, we have observed numerous nanometer sized cavities but a much smaller degree of amorphization. Heavy elements (Y , Lu. and Cm) are not present in the cavities at an observable concentration.

Sample preparation

The orthophosphate crystals doped with ^{244}Cm ions that we investigated were grown in 1980 at Oak Ridge National Laboratory (ORNL) [8] using a high temperature flux method. Pure lutetium oxide (Lu_2O_3) or yttrium oxide (Y_2O_3), mixed with 2.8% CmO_2 (by weight), were combined with lead hydrogen phosphate [$PbHPO_4$] as a flux and heated to ~1360 °C in a platinum crucible within a furnace. The system was cooled at 1 °C per hour down to 800 °C, and then rapidly quenched to room temperature. This yielded single crystals of Cm^{3+}:$LuPO_4$ (or Cm^{3+}:YPO_4) with approximate dimensions of 0.5 mm x 1.0 mm x 4.0 mm and Cm^{3+} ion concentration of -1%. While some of the crystals were studied immediately after the growth process in electron paramagnetic resonance experiments [8,9], the samples that we studied were initially kept in a storage room at ORNL and shipped to ANL in 1993. After 17 years of accumulated radiation damage, the crystals are no longer transparent. Under an optical microscope, colored stripes are observable that range from dark brown to gray and run along the crystal's c-axis. Because ^{244}Cm is an alpha particle emitter with a relatively short lifetime and rarely fissions (spontaneous fission half-life: 1.34×10^7 y), alpha decay is the preponderant source of accumulated radiation damage in these crystals. For comparison purposes, we have also studied non-radioactive crystals of $LuPO_4$ and YPO_4 that contain ~1% Eu^{3+} ions and were grown by the same method.

Amorphization

Electron diffraction images of the ^{244}Cm:$LuPO_4$ samples that were recorded during this project show evidence of lattice disordering (partial amorphization). As shown in Fig. 1, the regular pattern of electron diffraction spots arises from the remaining crystalline lattice and diffuse diffraction spots and rings arise from amorphization of the lattice. In addition, some irregular sports also appear in the ED image, which suggests the presence of domains of crystalline lattice that have different orientations. In comparison with the ED image of the undamaged crystalline lattice of Eu:$LuPO_4$ that is shown in Fig. lb, the original crystalline lattice of Cm:$LuPO_4$ obviously has been altered to a certain degree, but is far from complete amorphization.   This observation is

inconsistent with the collision model that is widely used in the literature for calculation of ion implantation induced amorphization and alpha decay induced lattice damage in solids[10,11].

In a a-decay event, the a-particle and the u-recoil nucleus are travel in opposite directions and produce distinctly different damaged regions. Based on the collision model and related calculations [5-7], a cc-particle produces several hundred well-separated atomic displacements along its path which ranges over ~20 μm. The more massive, but lower energy, associated a-recoil nucleus produces ~2000 atomic displacements in a more localized region (30 to 40 nm diameter). Based on this estimation, complete amorphization of the 1% Cm in $LuPO_4$ crystal should have occurred when 5% -10 % of the initially present [244]Cm ions decayed into [240]Pu. Given a half lifetime of 18.1 years, only 2 years would be required reach complete amorphization. However, after 17 years, a large portion of the lattice in a 1% Cm in $LuPO_4$ crystal is still crystalline.
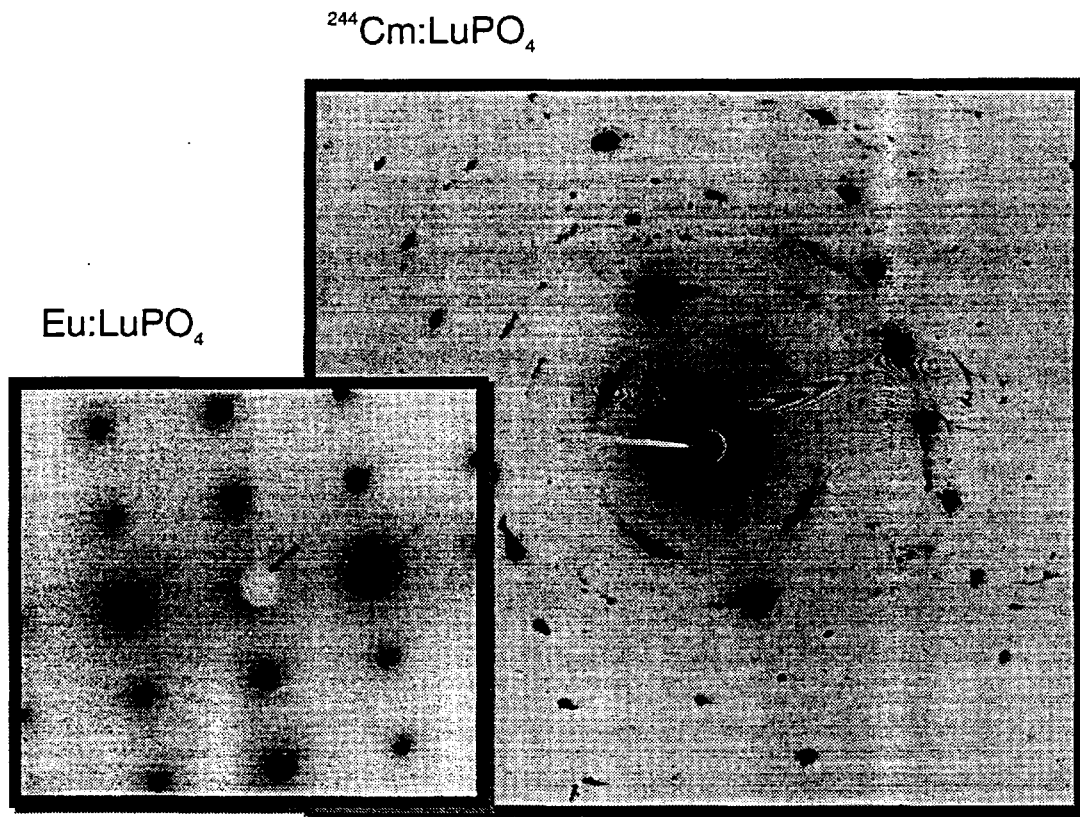
[244]Cm:LuPO$_4$

Eu:LuPO$_4$

Fig. 1 Comparison of electron diffraction patterns of radiation damaged crystal of [244]Cm:LuPO$_4$ and undamaged crystal of Eu:LuPO$_4$. The images were recorded with the electron beam propagating approximately along the c-axis of the crystal.

At present, we have no definitive interpretation for this discrepancy. As previously has suggested by others, one possibility is that the orthophosphates have the ability to self-anneal at low temperature relative to their melting point. If this is true, then most of the alpha decay induced damage in the 17-year old ^{244}Cm:LuPO$_4$ samples evidently has self-annealed at room temperature. Such a "radiation resistant" property would then make orthophosphates a very attractive high level nuclear waste form. However. further research is needed before we can draw a final conclusion as the source of this difference between past collision model predictions and our experimental observations.

Formation of nanocavities

The most interesting, and perhaps technically important, observation made in our one year of research activities is the discovery of nanometer scale cavities (or bubbles) in the 17 year old ^{244}Cm^{3+}:LuPO$_4$ crystalline samples. In transmission electron microscopic (TEM) images of samples whose thickness was reduced to ~ 100 nm prior to imaging, irregularly distributed cavities of ~ 10 nm dimension are evident, as seen in Fig. 2, whereas in the regions surrounding the cavities, the crystalline structure is clearly less
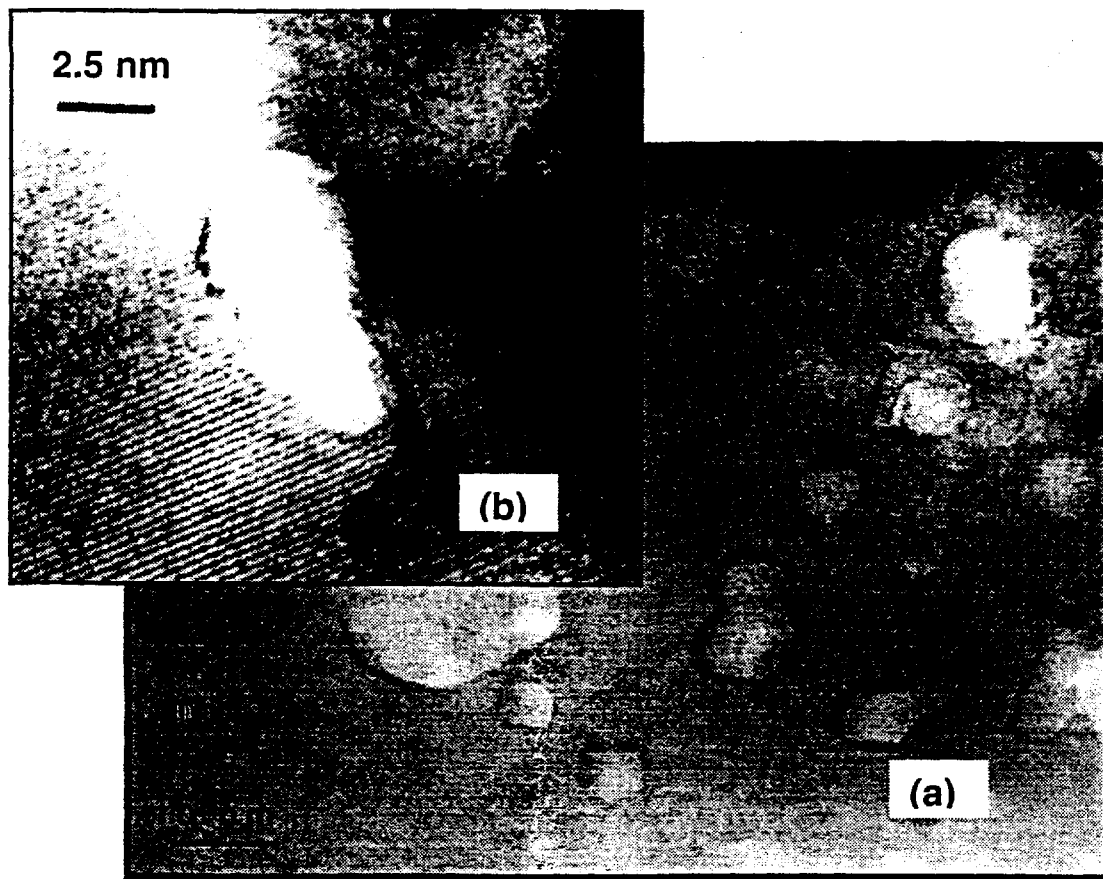

Fig. 2 TEM images of a 17-year old sample of LuPO$_4$ containing ~1% ^{244}Cm. Numerous nanometer scale cavities are observable in (a) throughout the sample, whereas a large portion of the sample still has crystalline structure and (b) is an increased magnification image that shows a cavity surrounded by less damaged crystalline lattice.

damaged. Regions of preserved crystalline structure are clearly evident in a magnified portion of the TEM image (Fig. 2 b) which shows a cavity formed in a crystalline domain. A non-radioactive single crystal of $LuPO_4$ doped with 1% Eu^{3+} was also studied using the TEM and ED methods. No evidence of cavities or other types of microscopic structural defects were found.

In general, the observed structural damage induced by alpha-particle emission of ^{244}Cm may be understood based on the anisotropic dislocation of atoms within the orthophosphate structure. Alternatively, the observed effects may be interpreted by assuming a non-uniform distribution of ^{244}Cm ions in the sample. The ^{244}Cm concentration in some regions might be much higher than that in other regions. In such ^{244}Cm ion aggregated regions, severe radiation damage may have created the observed cavities. It is speculated that the cavities contain helium and oxygen gasses. Whereas helium gas would arise from trapped alpha particles, it is possible that oxygen atoms are released as a consequence of chemical decomposition. Bubbles containing oxygen previously were observed in radiation damaged borosilicate glasses [12,13]. The possibility of finding heavy elements in the cavities is unlikely due to the fact that images of cavities appear much brighter than that of the surrounding regions and therefore are regions of lower electron density.

Experimental identification of the chemical composition of the different regions, particularly in the cavities, is very important for understanding the self radiation induced structure damage and chemical decomposition. Further studies also are needed to determine the thermal annealing dynamics of the damaged phases. While the nano-cavities are unlikely to be recrystalizable, it is anticipated that, at sufficiently elevated temperature, some of the amorphous regions and the less damaged crystal lattice areas will recrystalize into the original $LuPO_4$ structure.

Structural Disordering Probed via Laser Spectroscopy

Sections of 17-year old crystals of $^{244}Cm:LuPO_4$ and $^{244}Cm:YPO_4$ have been studied with high resolution laser spectroscopic methods. Site-selected laser excitation and energy-resolved fluorescence detection methods, also known as fluorescence line narrowing [14,15], were used effectively to obtain detailed information on structure disordering induced by alpha decay events in these aged samples.

The orthophosphate crystals $LuPO_4$ and YPO_4 have a body-centered tetragonal zircon-type structure [16]. An actinide ion substituting for a Lu^{3+} (or Y^{3+}) site has D_{2d} site symmetry. In consequence, all crystal field states of Cm f-electrons are two-fold degenerate (a J=7/2 free-ion state is split into 4 doublets) [16-18]. In the $^{244}Cm^{3+}:LuPO_4$ and $^{244}Cm^{3+}:YPO_4$ samples, the inhomogeneous line width that we measured for $^8S_{7/2} \leftrightarrow$ $^6D_{7/2}$ transitions of Cm^{3+} was 50 cm^{-1} or broader when using linear spectroscopic methods. We attribute this large line width to radiation damage in the 17 years since the crystals were grown. This result suggests that the local environment of Cm^{3+} ions in the studied samples has amorphized to a degree that lies between that of a perfect crystal

(where the line width would be less than 1 cm^{-1}) and a glass (where the line width would be larger than 100 cm^{-1}) [19-22]. Analysis of the site-selective laser induced fluorescence spectra indicates that the line broadening is microscopic in nature, which means that individual Cm^{3+} ions have different lattice environments. This is an expected consequence of a-decay damage. We have quantitatively characterized this effect via computer simulation of our laser experiments. Results from these simulations show that the microscopic crystalline damage is much less than that predicted by collision models that assume atom displacements that do not vary with accumulated radiation damage. However, our laser spectroscopy, electron microscopy, and computer modeling results are consistent with the conclusion that only partial amphorization with significant residual crystallinity is present in the [244]Cm-doped orthophosphate crystals after 17 years accumulation of radiation damage.

It is generally known that the optical spectrum of f-element ions in crystals provides "fingerprint" information about the local lattice structure [15,19,23]. The line broadening of optical transitions between crystal-field states of different electronic multiplets within an f-configuration arises from static crystalline defects. Studies of inhomogeneous line broadening, in principle, can provide information about the nature and distribution of defects in crystals [19,21, 23,24]. In our work, the electronic energy level structure of alpha-emitting isotope [244]Cm^{3+} doped into single crystals of $LuPO_4$ and YPO_4 has been studied using site-selective laser spectroscopic methods. Electronic transitions between the nominal $^8S_{7/2}$ ground state and the excited $^6D_{7/2}$ state of Cm^{3+} were utilized to characterize the effects of alpha-decay induced structural damage.

Experimental details

An argon ion laser pumped tunable CW dye laser with a band width of 0.07 cm^{-1} was the excitation source for recording fluorescence line narrowing (FLN) and excitation spectra. We use here the traditional spectroscopic unit of energy, the wave number, and note that 1 cm^{-1} = 1.24×10^{-4} eV. A monochromator with a spectral band pass of 0.3 cm^{-1} was used to select the fluorescence energy of the emission from the $^6D_{7/2}$ state. Fluorescence emission was detected by a cooled photomultiplier that was connected to a computer-interfaced lock-in amplifier. For FLN measurements, two acousto-optic modulators were used in series to convert the CW laser beam into a train of light pulses. A mechanical chopper that was synchronized with the modulators blocked residual. laser light while passing Cm^{3+} fluorescence. With this time-resolved pump-then-detect method, scattered laser light was discriminated against by more than a factor of 10^6 when recording fluorescence spectra.

Initial studies used a pulsed 355 nm laser as the excitation source. The observed line width of the $^6D_{7/2}$ fluorescence emission was broader than 50 cm^{-1} at temperatures below 10 K. When excitation of Cm^{3+} ions was induced by the modulated CW laser to the upper levels of the $^6D_{7/2}$ multiplet and subsequent fluorescence emission from the lowest doublet at 16570 cm^{-1} was monitored, the emission spectrum became narrower (see Fig. 3) and its line center shifted as a function of excitation energy. In these laser studies, fluorescence line narrowing was achieved only when the emitting state (the

lowest doublet of the $^6D_{7/2}$ multiplet) was directly excited. The narrow central peak is termed the resonant fluorescence line narrowed line or RFLN because it occurs at the same energy at which emission was monitored. Satellite lines were observed on both sides of the RFLN. These satellite lines are attributed to emission to the other 3 doublets of the ground multiplet. The emission arises from Cm^{3+} ions on sites that accidentally have the same excitation energy and from Cm^{3+} ions on others sites such that the excitation occurs from different ground state doublets. On this basis, a maximum of 12 satellite lines that are symmetrically spaced about the RFLN line may be observable. In a crystal of $LuPO_4$ doped with $^{244}Cm^{3+}$ ions, a FLN spectrum that included the RFLN line and 12 sharp satellite lines was indeed observed (see Fig. 4c). This confirms our interpretation and is attributed to the unusual energy level structure of Cm^{3+}. There is a difference in the number of observable lines in FLN spectra of Cm^{3+} in YPO_4 (see Fig. 3b) and Cm^{3+} in $LuPO_4$ (see Fig. 4c). This is attributed to the observed 1 cm^{-1} separation of the top two doublets in the $^8S_{7/2}$ ground state of Cm^{3+} in YPO_4 in comparison with a 1.5 cm^{-1} separation for Cm^{3+} in $LuPO_4$ and differences in inhomogeneous broadening of Cm^{3+} 5f state transitions between these two materials. In other respects, our laser spectroscopy results from these two materials are similar.
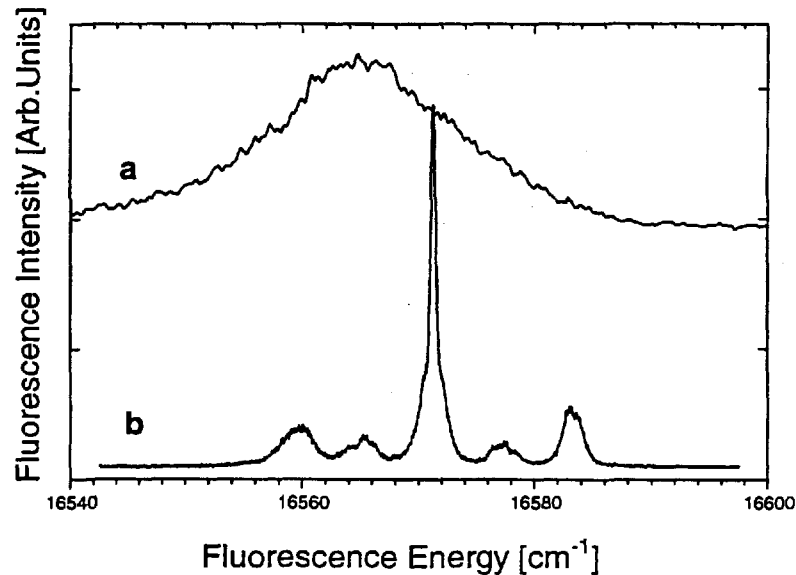

Fig. 3 Fluorescence spectra of Cm^{3+}:YPO_4 at 4 K The excitation was to $a)$ the second doublet at 16625 cm^{-1} and b) the lowest doublet at 16571 cm^{-1} of the $^6D_{7/2}$ excited state.

We have further observed that the FLN spectrum, consisting of a resonant line and a maximum of 12 satellite lines, varied dramatically as the laser excitation energy varied across the inhomogeneously broadened line center. The satellite lines became broader until they were indistinguishable as the excitation energy was tuned to higher or

lower energies about the line centered at 16570 cm^{-1} in YPO$_4$ and 16525 cm^{-1} in LuPO$_4$.
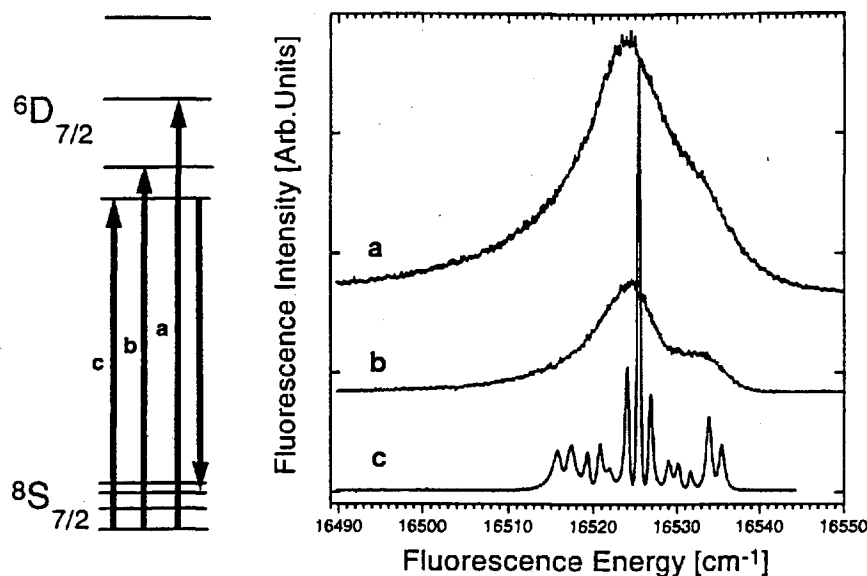

Fig. 4 Fluorescence spectra of Cm^{3+}:LuPO$_4$ at 4 K The excitation was to *a)* the third doublet at 16945 cm^{-1}, *b)* the second doublet at 16584 cm^{-1}, and *c)* the lowest (resonant) doublet at 16525 cm^{-1} of the ^{6}D$_{7/2}$ excited state.

Characterization of microscopic radiation damage

The line broadening for the ^{8}S$_{7/2}$ ground state to the ^{6}D$_{7/2}$ excited state transitions is mainly due to the crystal-field energy level shifts in the excited state. In the ^{8}S$_{7/2}$ state, the measured total crystal-field splitting is only 10 cm^{-1} in LuPO$_4$, and 12.5 cm^{-1} in YPO$_4$ because the interaction matrixes involving the ^{8}S$_{7/2}$ free-ion state vanish in the ground multiplet. The observed splitting is due to higher order coupling mechanisms that induce mixing of the excited state wave functions into the ground multiplet [16-18, 25]. For the ^{6}D$_{7/2}$ excited state, first order crystal field coupling is the leading mechanism for free-ion energy level splitting as well as for inhomogeneous line broadening. A total splitting of more than 600 cm^{-1} was observed for the ^{6}D$_{7/2}$ multiplet of Cm^{3+} ion in both compounds. As a result, the inhomogeneous line broadening of the ^{8}S$_{7/2}$ ↔ ^{6}D$_{7/2}$ transitions is dominated by the crystal field energy level variation in the excited state. The effect of radiation damage-induced structural changes on the electronic energy level structure of C m^{3+} is not significant in its ground state. This conclusion is supported by the observation of as many as 12 symmetrically spaced satellite lines in FLN spectra that were recorded as the laser wavelength was varied across the center of the inhomogeneously broadened line. This special electronic property of Cm^{3+} allows us to use the inhomogeneous line width of the ^{8}S$_{7/2}$ ↔ ^{6}D$_{7/2}$ transitions to characterize the

crystal field energy level variation and thereby link energy level variation to the crystalline damage.

As shown in Figs. 3 and 4, sharp lines were observed only in FLN spectra. Laser excitation of Cm^{3+} into any of the crystal field doublets or vibronic states above the lowest crystal field doublet did not result in narrow emission lines, although the shape and location of the line center varied for different excitation energies (see Figs. *4a* and *4b)*. Since phonon-induced broadening at 4 K should be much less than the observed line width and the laser band width is also negligible, the excitation energy dependent emission spectra shown in Fig. 4 suggest that structure damage induced variation in the crystal field energy levels of the $^6D_{7/2}$ state is not correlated between different crystal field doublets. Selected by a narrow band laser, a set of Cm^{3+} ions on different sites that accidentally give rise to ions that have the same excitation energy between the ground state and one of the four crystal field doublets of the $^6D_{7/2}$ excited multiplet may have different energies for transitions into other states. This suggests that a set of Cm^{3+} ions that have different solid state environments may coincidentally have the same transition energy in the upper states of the $^6D_{7/2}$ multiplet. This accidental degeneracy is removed as the ions nonradiatively relax into the lower emitting doublet. The broad emission spectrum thus represents the energy level differences in the excited state.

Because the inhomogeneous line width is broader than the total splitting of the ground state due to the much larger crystal field interaction in the $^6D_{7/2}$ excited state, simultaneous excitation of Cm^{3+} ions of different excitation energies (due to different local environments) is possible at a given laser energy. To be excited at the same laser energy, Cm^{3+} ions must be from different doublets in the ground state. The maximum difference in excitation energy for Cm^{3+} ions in different local environments therefore must not exceed the total splitting of the ground state of Cm^{3+}. Thus, one group of Cm^{3+} ions is excited from the lowest level of the ground state, another group is excited from the second level of the ground state, and so on. Subsequently, each of the four groups produces four emission lines. The observed central RFLN line has 4 fold degeneracy (its intensity is about 4 times of that of satellite lines) and there are, therefore, a maximum of 12 satellite lines that can be observed symmetrically spaced about the RFLN line.

The spectroscopic properties of $^{244}Cm^{3+}$ ions in the 17-year old YPO_4 and $LuPO_4$ crystals are different from those of trivalent ^{248}Cm ($t_{1/2} = 4.7 \times 10^5$ y) in the similar crystals. In the case of $^{248}Cm^{3+}$ doped crystals, the inhomogeneous line broadening of optical transitions is less than the ground state splitting which reduces the number of satellite lines that are observable in an FLN spectrum [16-18]. In the case of $^{248}Cm^{3+}$ ions in glasses, inhomogeneous line broadening is much larger than 100 cm^{-1} and no sharp satellite lines were observable [21]. This suggests that the degree of disorder induced by alpha decay damage in the YPO_4 and $LuPO_4$ crystals that we have studied is much greater than that induced by crystalline defects formed in crystal growth but less than that in a glass matrix. Although, after 17 years of alpha-decay damage, the surrounding lattices for most of the existing $^{244}Cm^{3+}$ ions may have undergone significant displacements and distortion, the nearest neighbor bonding and coordination, in particularly the structure of PO_4^{3-}, evidently has been left without severe damage [26].

Our observations also show that alpha decay induced structural damage is not uniform. More severe damage in the surrounding lattice of Cm^{3+} ions was evident in FLN spectra as the excitation energies were moved further away from the center of the inhomogeneous line profile. In this case, the FLN spectra showed no sharp satellite lines but only a broad wing on each side of the resonant line. Such spectra are characteristic of Cm^{3+} in amorphous phases such as glass [21].

Computer Modeling and Simulation

Computer simulation and modeling have played an important role in this project for achieving a thorough fundamental understanding of experimental observations. Accomplishments in this first year of our project include crystal field model calculation of observed spectra and Monte-Carlo simulation of alpha-decay events induced atomic position displacements (amorphization).

Simulation of structural disordering and the observed inhomogeneous spectral line broadening suggest that, for most of the existing Cm^{3+} ions in the samples of $^{244}Cm^{3+}:YPO_4$ and $^{244}Cm:LuPO_4$, the average displacements of lattice ions that surround a Cm^{3+} ion is about 0.2% ($8x10^{-4}$ nm) of the unit cell dimension. Because all of the ions in the lattice should have undergone atomic displacements induced by the alpha projectiles and recoiling nuclei and the expected displacements are much larger than $8x10^{-4}$ nm, this result argues that much of the alpha-decay induced lattice damage has been reversed by self-annealing.

Our calculation was based upon Cm^{3+}-lattice electronic interactions that strongly depend on the coordination and crystalline structure. For actinide ions in solids, the 5f electrons are localized and "weakly" coupled to the ligand field. As a result, optical transitions between 5f states give rise to sharp lines that carry information about local structure. This unusual electronic property also facilitates the calculation of 5f state energy level structure. We used the exchange charge model of crystal field interaction [27] and non-linear least squares fitting to extract structural information from the observed optical spectra. By taking the advantages of our established experience in crystal field modeling, we were able to calculate the energy levels of Cm^{3+} ions on displaced sites as well as on undamaged sites.

Successful theoretical calculation of crystal field energy level structure of actinide ions in disordered crystalline lattices enabled us to establish a quantitative correlation between structural disordering induced by radiation damage and the variation of the crystal field 'energy levels of a specific actinide element. With this quantitative correlation, an inhomogeneously broadened optical absorption or emission spectrum can be analyzed to gain information about local structure defects, and in our project, determine alpha-decay induced structural disordering in orthophosphate crystals. Whereas the simulation reproduced our optical experiments very well, the average displacement resulting from our Monte-Carlo calculations is only $8x10^{-4}$ nm. This suggests that the crystalline lattice is not significantly damaged, as is supported by the

ED and TEM imaging studies described earlier in this report. Fig. 5 schematically shows the simulated consequence of crystalline damage, based on our Monte Carlo calculations.
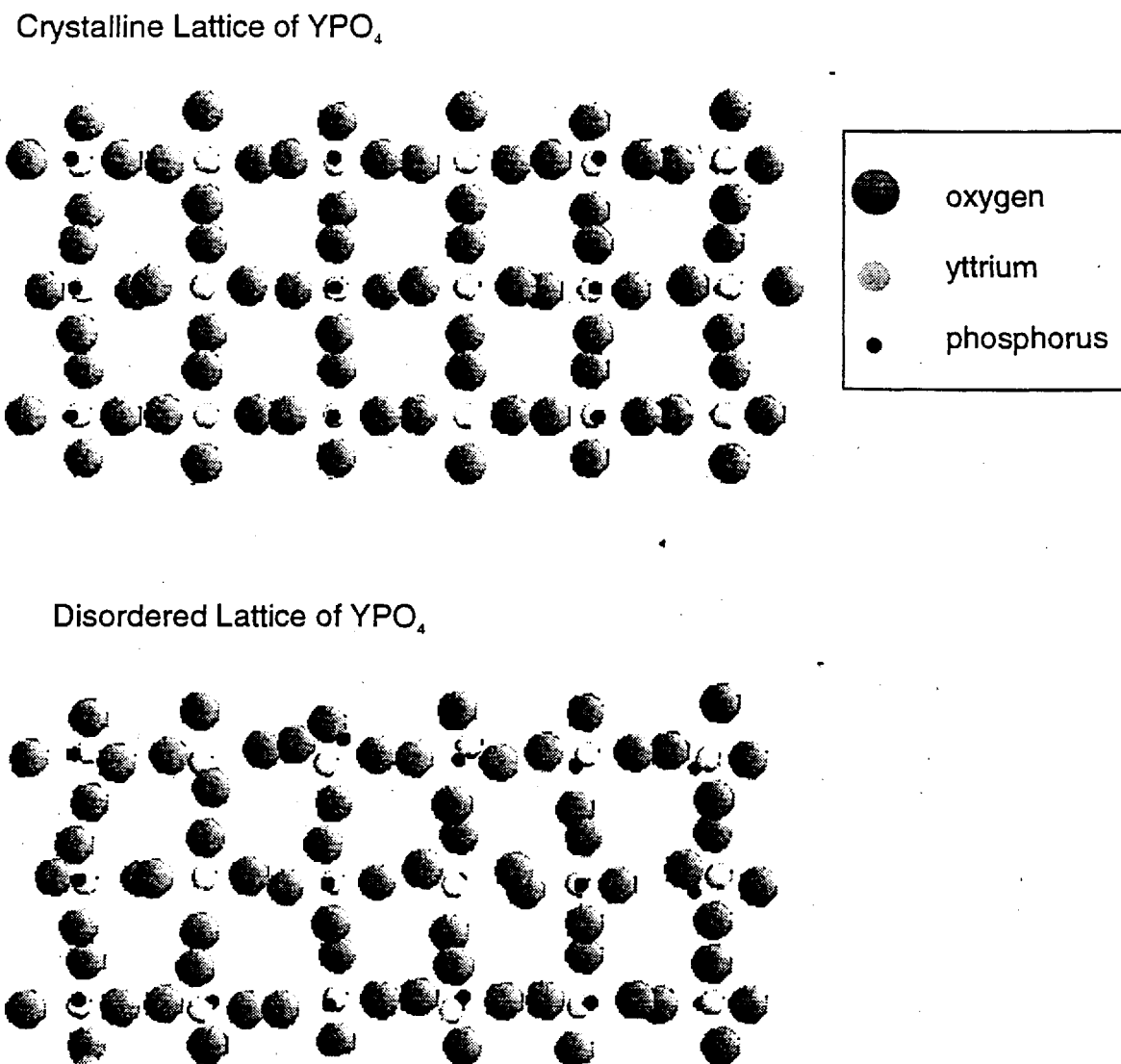
Crystalline Lattice of YPO_4

- ● oxygen
- ◉ yttrium
- • phosphorus

Disordered Lattice of YPO_4

Fig. 5   Monte Carlo simulation of atomic displacements in YPO_4. The upper part is a perfect crystalline lattice, and-the lower part is a layer of disordered lattice. The disordering drawn in this figure is 20 times larger than the actual disordering that simulates the experimental observation. Note that ion diameters are not drawn to scale.

Based on such damaged lattices, resonant and non-resonant fluorescence line narrowing spectra were simulated for Cm^{3+} ions in YPO_4, as shown in Fig.6, for comparison with experimental results such as those shown in Fig. 3.
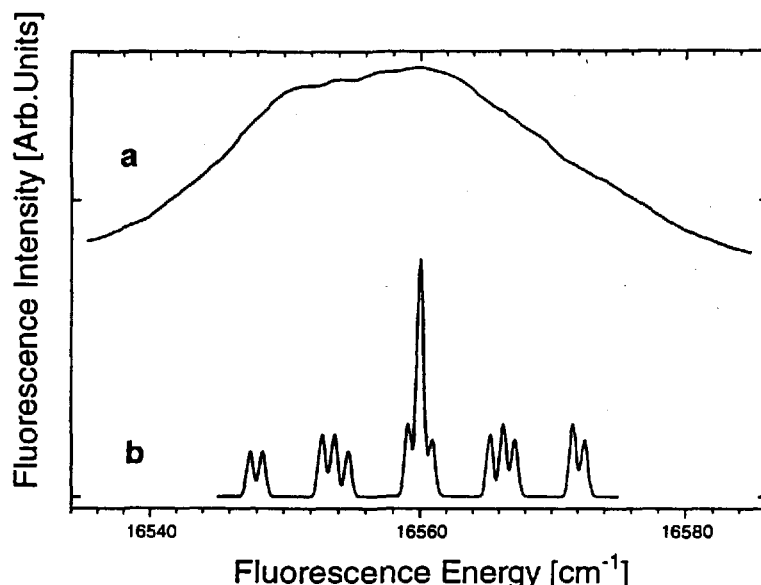

Fig. 6 Monte Carlo simulation of resonant and non-resonant fluorescence line narrowing spectra for Cm^{3+} ions in structure-disordered crystals of YPO_4. Considering fluorescence from the lowest doublet of the $^6D_{7/2}$ excited multiplet, (a) is for non-resonant excitation at 17181 cm^{-1} to the highest doublet of $^6D_{7/2}$, and (b) is for resonant excitation to the lowest doublet of the $^6D_{7/2}$ state at 16560 cm^{-1}.

Preparation of Borosilicate Glass Samples

Great emphasis in our project is placed on the studies of microscopic effects of radiation damage in glass with the bulk of this work to be carried out in the 2nd and 3rd years of our studies. Progress has been made in preparing borosilicate glass samples and their characterization. A new high temperature (1700 C) furnace was purchased for synthesizing glasses to be studied in this project and has been tested. A number of borosilicate glass samples have been prepared using this capability. The composition of these samples typically has been 72%SiO_2, 12 %BO_2O_3, 11% Na_2O, and 5% Al_2O_3, prior to heavy metal doping. These samples are to be ground, mixed with $^{241}AmO_2$ and $^{244}CmO_2$, respectively, and melted to simulate actual high level waste glasses. We have purchased 1.2 mg of ^{244}Cm from ORNL and will use ^{241}Am from existing radionuclide

inventories at ANL. The operational safety review requires the furnace be placed into a newly installed hood. The installation of the hood was delayed however by large scale renovation in the M-Wing of Building 200 where our hot chemistry labs are located. We expect that the preparation of actinide-doped borosilicate glass samples will be complete in October, 1997. Currently, we are studying glass samples doped with Eu^{3+} ions. Comparative studies on actinide and lanthanide doped glasses are critical in our project for fundamental understanding the microscopic effects of radiation damage.

Planned Work

More extensive investigation on the discrepancy between amorphization models based on collision-induced radiation damage and our experimental observations, the mechanisms of cavity formation, and the dynamics of thermal annealing of highly radiation damaged samples of $^{244}Cm:LuPO_4$ and $^{244}Cm:YPO_4$ will be conducted. All of our present experiments have been conducted at or below room temperature to avoid thermal annealing of existing accumulated radiation damage and to gather as much information as possible before we conduct thermal annealing tests and repeat our measurements.

A heating stage has been purchased and will be installed in the high resolution electron microscope for *in-situ* TEM and ED measurements while a sample is heated. In addition, with modification of the existing electron microscope, we will be able to obtain element selected TEM images that are crucial for determining the elements present in the observed cavities as well as the distribution of the remaining ^{244}Cm ions in our aged samples.

For laser spectroscopic studies, the ^{244}Cm-doped YPO_4 and $LuPO_4$ samples will be annealed at increasing temperature. Laser measurements will be repeated after each annealing step to probe microscopic changes in structure. Because $^{244}Cm^{3+}$ has no nuclear spin moment, our optically-detected nuclear magnetic resonance (ODNMR) technique cannot be applied to the bulk of the Cm ions present although we expect that electronic Zeeman effect studies on samples in a static magnetic field will prove useful. We will seek to carry out ODNMR measurements on the $^{243}Cm^{3+}$ ions present in the $LuPO_4$ samples. There is evidence of the presence of ^{243}Cm in our existing $^{244}Cm^{3+}:LuPO_4$ samples [8,9].

Analytical electron microscopy and laser spectroscopic experiments will be conducted immediately after the ^{241}Am and ^{244}Cm containing borosilicate glass samples are prepared. These experiments will be repeated at periodic interval thereafter to monitor the development and extent of radiation damage. In addition, experiments will be conducted on ThO_2 crystals that were originally doped with ^{249}Bk for investigation of beta decay induced damage. The ^{249}Bk initially-present largely has decayed to ^{249}Cf. Our computer modeling and simulation capability will be enhanced to establish more precisely the relationship between damaged lattices and observed optical spectra of actinide and other heavy element ions.

Publications and Submission

The following publications and submissions have resulted from this research project.

1. **Effects Of Radiation Damage On Electronic Properties Of Rare Earth Ions In Zircon**
   G. K. Liu, J. M. Hanchar, D. J. Cherniak and E. B. Watson
   APS Bulletin **42,** 98 (1997).

2. **Self-Radiation Induced Anisotropic Structure Damage In ^{244}Cm-Doped Orthophosphate LuPO$_4$**
   G. K. Liu, J. S. Luo, S. T. Li, C.-K. Loong, M. M. Abraham, J. V. Beitz, J. K. Bates, and L. A. Boatner
   Scientific Basis for Nuclear Waste Management, Volume 21, (submitted).

3. **Effects Of Self-Radiation Damage On Electronic Properties Of ^{244}Cm^{3+} In Orthophosphate Crystals Of YPO$_4$**
   G. K. Liu, S. T. Li, J. V. Beitz, and M. M. Abraham
   Journal of Alloys and Compounds (submitted).

Literature References

1. W. J. Weber, R. C. Ewing, C. A. Angell, G. W. Arnold, A. N. Cormack, J. M. Delaye, D. L. Griscom, L. W. Hobbs, A. Navrotsky, D. L. Price, and a. M. Stoneham, M. C. Weinberg, J. Mater. Res. **12,** 1946 (1997).

2. L. A. Boatner and B. C. Sales, in *Radioactive Waste Forms For the Future,* edited by W. Lutze and R. C. Ewing (Elsevier, Amsterdam, 1988) pp. 495-564.

   L. A. Boatner, G. W. Beall, M. M. Abraham, C. B. Finch, P. G. Huray, and M. Rappaz, in *Scientific Basis for Nuclear Waste Management, Vol. 2,* edited by C. J. M. Northrup Jr. (Plenum, New York, 1980), pp 289-296.

3. R. C. Ewing, W. Lutz, and W. J. Weber, J. Mater. Res. **10,** 243(1995).

4. B. E. Burakov, E. B. Anderson, V. S. Rovsha, S. V. Ushakov, R. C. Ewing, W. Lutz, and W. J. Weber, in *Scientific Basis for Nuclear Waste Management XIX,* edited by W. M. Murphy and D. A. Knecht (Plenum, New York, 1996), pp 33-40.

5. W. J. Weber, and F. P. Roberts, **Nucl. Tee. 60,** 178(1983).

6. L. M. Wang, R. C. Ewing, and W. J. Weber, in *Pro. Microscopy and Microanalysis,* edited by G. W. Bailey, M. H. Ellisman. R. A. Henniger, and N. J. Zaiuzec, (Jones&Begell, New York, 1995).

7. G. L. McVay, W. J. Weber, and L. R. Pederson, Nucl. Chem. Waste Mgmt. **2,** 103(1981).

8. M. M. Abraham and L. A. Boatner, Phys. Rev. **B26,** 1434(1982).

9. M. M. Abraham, L. A. Boatner, C. B. Finch, W. K. Kot, J. G. Conway, G. V. Shalimoff, and N. M. Edelstein, Phys. Rev. **B35,** 3057(1987).

10. J. F. Gibbons, Proc. IEEE **60,** 1062 (1972).

11. W. J. Weber, R. C. Ewing, and L. M. Wang, J. Mater. Res. **9,** 688 (1994).

12. W. J. Weber, Nucl. Inst. Meth. & Meth. In Phys. Res. **B32,** 471(1988).

13. J.F. DeNatale, D.G. Howitt, and G.W. Arnold, Radiation Effects **98,** 63(1986).

14. Macfarlane, R.M. and R.M. Shelby, J. Lumin. **36,** 179 (1987).

15. Macfarlane, R.M. and R.M. Shelby, in *Spectroscopy of solids containing rare earth ions,* eds A.A. Kaplyanskii and R.M. Macfarlane (North-Holland, New York 1987) Chapter 2.

16. W. K. Kot, N. M. Edelstein, M. M. Abraham, and L. A. Boatner, Phys. Rev. **B48,** 12704(1993).

17. J. Sytsma, K. M. Murdoch, N. M. Edelstein, L. A. Boatner, and M. M. Abraham, Phys. Rev. **B52,** 12668(1995).

18. K. M. Murdoch, N. M. Edelstein, L. A. Boatner, and M. M. Abraham, J. Chem. Phys. **105,** 2539(1996).

19. B. B. Laird and J. L. Skinner, J. Chem. Phys. **90,** 3880(1990).

20. G. K. Liu, Jin Huang, and J. V. Beitz, Phys. Rev. **B48,** 13351(1993).

21. R. T. Brundage, R. L. Powell, J. V. Beitz, and G. K. Liu, J. Lumin. **69,** 121(1996).

22. G. K. Liu, J. V. Beitz, and J. Huang, J. Chem. Phys. **99,** 3304(1993).

23. Yen, W.M. and P.M. Seizer, in *Laser Spectroscopy of Solids,* eds W.M. Yen and P.M. Selzer (Spinger, New York 1981) Chapter 5.

24. Yen, W.M., in *Spectroscopy of Solids Containing Rare Earth Ions,* eds A.A.

Kaplyanskii and R.M. Macfarlane (North-Holland, New York 1987) Chapter 4.

25. B. G. Wyboume, Phys. Rev. **148,** 317(1966).

26. J. A. Woodhead, G. R. Rossman, and L. T. Silver, American Mineralogist **76,** 74(1991).

27. B.Z. Malkin, in *Spectroscopy of Solids Containing Rare Earth Ions,* edited by A.A.Kaplyanskii and R.M.Macfarlane, (North-Holland, Amsterdam, 1987) p. 13.